G Stankunas et al.

# Measurements of fusion neutron yields by neutron activation technique: uncertainty due to the uncertainty on activation cross sections

# Measurements of fusion neutron yields by neutron activation technique: uncertainty due to the uncertainty on activation cross sections

Gediminas Stankunas[a], Paola Batistoni[b], Sean Conroy[c], and JET Contributors[*]

***EUROfusion Consortium, JET, Culham Science Centre, Abingdon, OX14 3DB, UK***

[a]*Lithuanian Energy Institute, Laboratory of Nuclear Installation Safety, Breslaujos str. 3, LT-44403 Kaunas, Lithuania*
[b]*ENEA, Via E. Fermi,45, 00044 Frascati,(Rome) Italy*
[c]*Department of Physics and Astronomy, Uppsala University, P.O. Box 516, SE-75120 Uppsala, Sweden*

The neutron activation technique is routinely used in fusion experiments to measure the neutron yields. This paper investigates the uncertainty on these measurements as due to the uncertainties on dosimetry and activation reactions. For this purpose, activation cross sections were taken from the International Reactor Dosimetry and Fusion File (IRDFF-v1.02) in 640 groups ENDF-6 format for several reactions of interest for both 2.5 and 14 MeV neutrons. Activation coefficients (reaction rates) have been calculated using the neutron flux spectra at JET vacuum vessel, both for DD and DT plasmas, calculated by MCNP in the required 640-energy group format. The related uncertainties for the JET neutron spectra are evaluated as well using the covariance data available in the library. These uncertainties are in general small, but not negligible when high accuracy is required in the determination of the fusion neutron yields.

Keywords: fusion neutron yield, activation technique, uncertainty of dosimetric cross sections

## Introduction

The neutron activation system plays an important role in the measurements of the absolute neutron yield and in the calibration of neutron detectors in fusion experimental devices [1, 2, 3]. It relies on the measurement of the neutron induced activity in foils of suitable materials exposed to the neutron source, from which the local activation coefficient (reaction rate)

$$R = \langle \sigma \phi \rangle = \int \sigma(E)\Phi(E)dE, \tag{1}$$

can be derived, where $\sigma(E)$ is the cross section of the activation reactions used, $\phi(E)$ is the local neutron fluence and E is the neutron energy.

The local neutron fluence spectrum, in turn, can be related the to the neutron source intensity Y by means of neutron transport calculations:

$$Y = K\int \sigma(E)\Phi(E)dE, \tag{2}$$

where K is a constant which depends on the foils position during irradiation, the neutron source shape, position and energy spectrum. This method requires the accurate knowledge of activation cross sections $\sigma$ as the uncertainty on cross sections propagate directly in the uncertainty in the neutron yield measurements.

Neutron activation systems can be experimentally calibrated using neutron sources, such as $^{252}$Cf sources or neutron generators of well known intensity and energy spectrum. However, neutronics calculations are needed to derive the activation coefficients for the extended volume and energy spectrum of neutrons produced by the plasma source.

Whenever possible, dosimetric reactions with well-known cross sections are used. Usually, the uncertainty in such cross section is considered negligible, and therefore neglected, in the evaluation of the total uncertainty in the activation measurements. However, whenever high accuracy is desired the uncertainty on activation cross sections has to be considered. Moreover, specific applications in fusion devices may require the use of non dosimetric reactions:

a) high energy threshold activation reactions leading to the production of short lived gamma emitting nuclides are desired for neutron emission rate measurements with sufficient time resolution;

b) however, during neutron detector calibration procedures, when neutron sources with limited intensity are used, high energy threshold activation reactions leading to the production of gamma emitting nuclides with longer decay times are desirable to allow longer exposure and avoid saturation of activity;

c) several activation reactions with different energy thresholds are needed to discriminate the different fusion sources (such as DT neutrons from triton burn up in DD plasmas) and features of the local neutron spectrum at irradiation positions;

d) pure TT plasma could be explored for which the energy spectrum of neutron emission is poorly known. The activation system could complement the spectroscopic measurements provided that suitable activation cross section are available with energy threshold in the range 3 - 14 MeV.

The objective of the present work is to assess the contribution to the total uncertainty in the neutron yield which is due to the uncertainty in the activation cross sections in a fusion neutron spectrum. To this purpose, the case of the Joint European Torus (JET) has been investigated for both DD and DT plasmas, producing 2.5 and 14 MeV neutrons, respectively.

JET is presently the world's largest nuclear fusion research facility. It plays an important role in preparing

the operations on the future world's largest tokomak, ITER. In 2010 JET wall was replaced by the ITER-like wall (ILW) made of Beryllium, Tungsten and Tungsten coated on Carbon. The replacement of wall, as well as other significant modifications occurred in time, affected the neutron yield measurements which are the basis for the determination of the absolute fusion reaction rate.

For this reason, a new calibration of the JET neutron detectors at 2.5 MeV neutron energy, including external fission chambers (KN1) and the activation system (KN2), was performed using a $^{252}$Cf source deployed in many toroidal and poloidal position inside the vacuum vessel [4]. Moreover, as a new DT experimental campaign (DTE2) is planned at JET, the neutron detectors, fission chamber and activation system, will have to be calibrated at 14 MeV neutron energy using a well calibrated and characterized DT neutron generator [5]. In that campaign, also operations with a pure T plasma are planned.

In ITER, the absolute calibration of neutron detectors also relies upon the experimental calibration of the activation system using a DT neutron generator deployed in vessel at many toroidal/poloidal positions [6]. In both JET and ITER case, the target accuracy for the neutron calibration is better than ±10%.
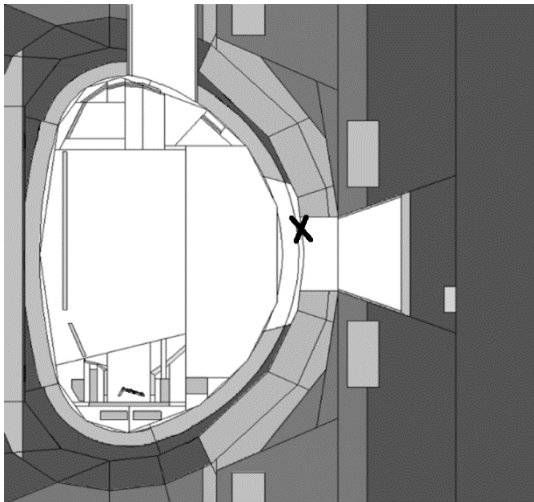


Figure 1. Poloidal section of JET tokamak. The neutron spectra are calculated in the area marked by X.

In the present work, the activation reactions and fission reactions currently in use at JET have been considered, as well as new ones that could be used in the future in view of DTE2. The activation reactions and the related uncertainties were taken from the International Reactor Dosimetry and Fusion File (IRDFF) [7] in 640 groups ENDF-6 form. IRDFF is a standardized evaluated cross section library of neutron dosimetry reactions with uncertainty information that supersedes a widely used IRDF-2002 library [8]. The IRDFF contains cross section data and related decay data for 74 dosimetry reactions, and absorption data for three cover materials B, Cd and Gd used during the irradiation of some specific detectors.

Activation coefficients (reaction rates) have been calculated using the neutron flux spectra at the JET vacuum vessel, both for DD and DT plasmas, in the required 640-energy group form and using cross sections available from the dosimetric library IRDFF-v1.02. The

related uncertainties for the JET neutron spectrum are evaluated as well using the covariance data available in the library. To this purpose, the RR_UNC code that reads spectra, cross sections (in 640-group form) and covariances to calculate the uncertainties, have been used. This code was provided by IAEA [9].

## Activation reactions and cross section covariance data

The cross sections of activation reactions and fission reactions currently in use at JET KN1 and KN2 are the following:

- DD plasmas: $^{115}$In(n,n')$^{115m}$In, $^{235}$U(n,f), $^{232}$Th(n,f);
- DT plasmas: $^{28}$Si(n,p)$^{28}$Al, $^{63}$Cu(n,2n)$^{62}$Cu, $^{238}$U(n,f), $^{56}$Fe(n,p)$^{56}$Mn;
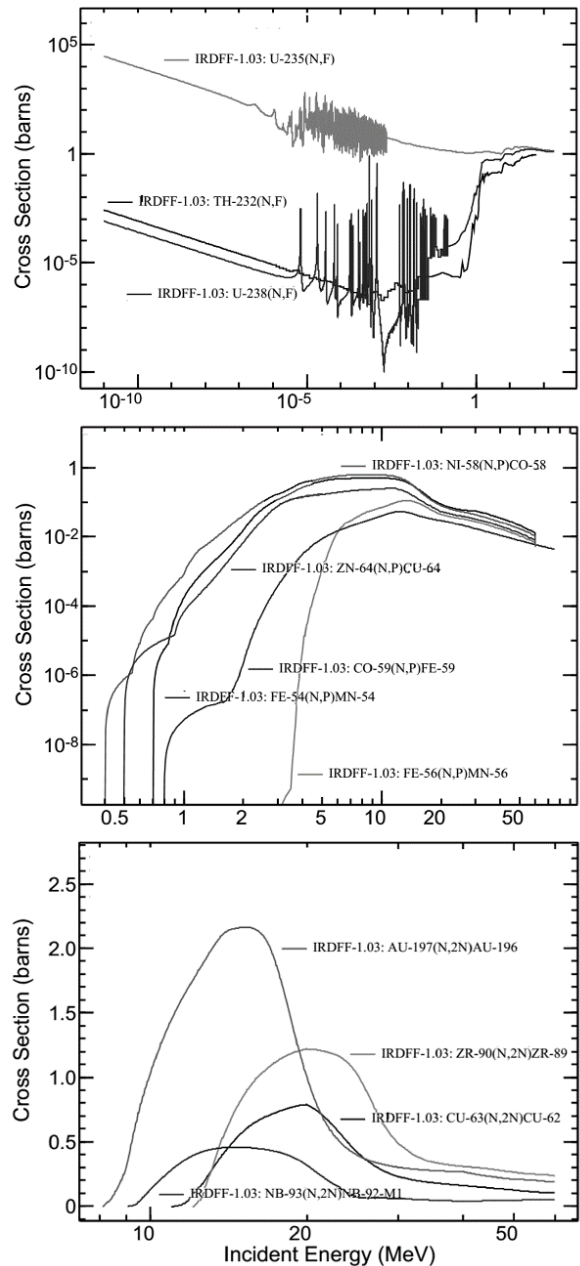


Figure 2. Cross-sections for selected reactions [10].

Other reactions could be used for applications such as those described in b) - d) in the Introduction, requiring e.g.

different energy thresholds in the range 3 to 14 MeV. The suitable reactions for these investigations are the following:

- calibrations for DD plasmas: $^{58}$Ni(n,p)$^{58}$Co, $^{64}$Zn(n,p)$^{64}$Cu, $^{54}$Fe(n,p)$^{54}$Mn;
- calibrations for TT plasmas: $^{59}$Co(n,p)$^{59}$Fe, $^{28}$Si(n,p)$^{28}$Al, $^{56}$Fe(n,p)$^{56}$Mn, $^{27}$Al(n,α)$^{24}$Na, $^{197}$Au(n,2n)$^{196}$Au;
- calibrations for DT plasmas: $^{63}$Cu(n,2n)$^{62}$Cu, $^{93}$Nb(n,2n)$^{92m}$Nb, $^{58}$Ni (n,2n)$^{57}$Ni, $^{90}$Zr(n,2n)$^{89}$Zr;

It should be noted that the in IRDFF new evaluation were provided for the following reactions: $^{235}$U(n,f), $^{238}$U(n,f), $^{232}$Th(n,f), $^{115}$In(n,n')$^{115m}$In, $^{64}$Zn(n,p)$^{64}$Cu, $^{54}$Fe(n,p)$^{54}$Mn, $^{27}$Al(n,α)$^{24}$Na, $^{63}$Cu(n,2n) $^{62}$Cu, $^{90}$Zr(n,2n)$^{89}$Zr, while the IRDF2002 evaluations were retained in IRDFF for $^{56}$Fe(n,p)$^{56}$Mn, $^{58}$Ni(n,p)$^{58}$Co.

All considered reactions and related decay data are summarized in Table 1, while selected cross-sections are provided in Fig.2 The following reactions are not used as dosimetric reactions and are not included neither in IRDFF nor in IRDF2002: $^{28}$Si(n,p)$^{28}$Al, $^{58}$Ni(n,2n)$^{57}$Ni.

However, given the interest of the $^{28}$Si(n,p)$^{28}$Al reaction for fusion experiment (relatively high cross section, and short half life of product = 2.24 minutes), this reaction has been recently evaluated by the IRDFF Project and included in the most recent IRDFF-v1.05 release [7], and it has been included in the present work.

Uncertainties on cross section measurements are due to statistical uncertainty (representing scatter among data) and systematic errors. In cross section evaluations using nuclear models, uncertainties are due to model approximations and deficiencies. In nuclear data libraries, these uncertainties are expressed in terms of covariances: the covariance matrix of cross sections is a matrix whose element in the (g,g') position is the covariance between the values of cross section in the $g_{th}$ and $g'_{th}$ energy groups. The covariance measures the correlation between the two values of the cross section in the two energy groups. The diagonal term of energy-energy covariance matrix are cross section uncertainties.

Folding the cross section of a reaction with a given neutron spectrum provides the reaction rate in that spectrum per target nucleus. When both the cross section and the neutron flux are defined in a given energy group form, the reaction rate is given by:

$$R = \sum_g \sigma_g \Phi_g, \qquad (3)$$

while the effective cross section in the given spectrum is defined as:

$$\langle \sigma \rangle = \frac{\sum_g \sigma_g \Phi_g}{\sum_g \Phi_g}. \qquad (4)$$

Folding the cross section covariance matrix with a given neutron spectrum provides the uncertainty on the reaction rate in that spectrum:

$$\frac{\delta R}{R} = \frac{\delta(\sigma \cdot \Phi)}{R} = \frac{1}{R}\left( \sqrt{(\sigma \cdot \Phi)^T \cdot \left\langle \left(\frac{\delta \sigma}{\sigma}\right)^T \left(\frac{\delta \sigma}{\sigma}\right) \right\rangle (\sigma \cdot \Phi)} + \langle \delta \Phi \cdot \sigma \rangle \right) = \frac{1}{\sum_g \sigma_g \Phi_g}\left( \sqrt{\sum_{g,g'} \sigma_g \Phi_g \cdot M\,\mathrm{cov}(\sigma)_{g,g'} \cdot \sigma_g \Phi_{g'}} + \sqrt{\sum_g \left(\sigma_g \cdot \delta \Phi_g\right)^2} \right),$$

$$(5)$$

where $M\,\mathrm{cov}(\sigma)$ is the relative covariance matrix as provided in the IRDFF file. Here also the contribution of the uncertainty on the neutron spectrum $\delta \Phi_g$ has been considered.

Table 1. Investigated reactions and their properties. Nuclear data are taken from [10].

| Reaction | Energy Threshold (MeV) | Gamma Ray Energy (keV) | Probability of emission (%) | Half life |
|---|---|---|---|---|
| $^{235}$U(n,f) | - | - | - | - |
| $^{238}$U(n,f) | ~1.0 | - | - | 1 min |
| $^{232}$Th(n,f) | ~1.2 | - | - | 1 min |
| $^{115}$In(n,n')$^{115m}$In | 0.5 | 336.241 | 45.8 | 4.486 d |
| $^{58}$Ni(n,p)$^{58}$Co | 1.0 | 810.7593 | 99.45 | 70.86 d |
| $^{64}$Zn(n,p)$^{64}$Cu | 1.8 | 511.0 | 35.2 | 12.701 h |
| $^{54}$Fe(n,p)$^{54}$Mn | 1.8 | 834.848 | 99.976 | 312.05 d |
| $^{59}$Co(n,p)$^{59}$Fe | 3.0 | 1099.245 | 56.5 | 44.495 d |
| $^{28}$Si(n,p)$^{28}$Al | 4.5 | 1778.85 | 100 | 2.24 min |
| $^{56}$Fe(n,p)$^{56}$Mn | 4.5 | 846.7638 | 98.85 | 2.58 h |
| $^{27}$Al(n,α)$^{24}$Na | 5.4 | 1368.626 | 99.99 | 14.997 h |
| $^{197}$Au(n,2n)$^{196}$Au | 8.5 | 188.27 | 30% | 9.6 h |
| $^{93}$Nb(n,2n)$^{92m}$Nb | 9.0 | 934.44 | 99.15 | 10.25 d |
| $^{63}$Cu(n,2n) $^{62}$Cu | 11.3 | 511.0 | 195.66 | 9.67 min |
| $^{58}$Ni (n,2n)$^{57}$Ni | 12.5 | 1337.6 | 81.7 | 35.6 h |
| $^{90}$Zr(n,2n)$^{89}$Zr | 13.0 | 909.15 | 99.04 | 78.4 h |

## JET neutron spectra and calculations of reaction rates and related uncertainties

The effective cross sections and the related uncertainties were calculated using Eqs. 3 and 4 and the JET neutron spectra. The RR_UNC code, provided by IAEA [9], was used. This code reads spectra, cross sections (in 640-group form) and covariances to calculate the uncertainties according to Eq.5. In these calculations, $\delta\Phi_g = 0$ was assumed, as the main purpose was to calculate the uncertainty $\delta R$ due to the uncertainties in the dosimetric cross sections $\delta\sigma$.

The same code had been previously used to validate the IRDFF covariance data in reference neutron fields: Maxwellian thermal, 1/E and $^{252}$Cf and for comparison with IRDF-2002. The reaction rates and related uncertainties for these reference fields using both IRDFF and IRDF-2002 data are given in [7-8].

As a first step, the $^{252}$Cf neutron spectrum was used to calculate cross-sections and related uncertainties. These results were compared with those presented in [8] in order to validate our procedure. The comparison showed perfect agreement (see Table 2 for details). The used $^{252}$Cf spectrum is also shown in Fig. 3.
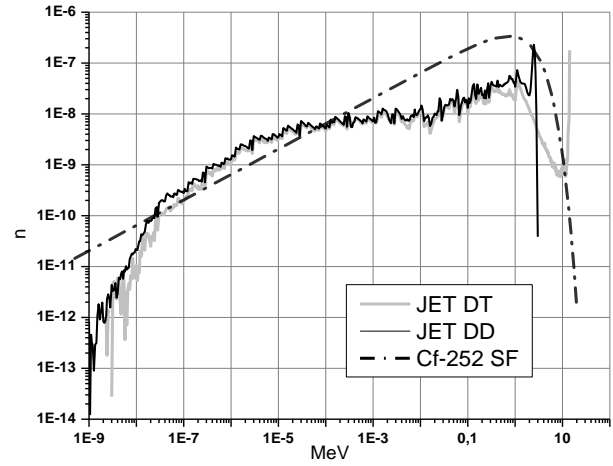


Figure 3. JET DT and DD neutron spectra at outboard midplane vacuum vessel together with $^{252}$Cf spontaneous fission neutron spectrum

In the next step, the calculations have been have extended to JET neutron fusion spectra. In order to start calculations using RR_UNC code, the spectra had to be calculated in ENDF 640-group form by MCNP for the input. JET spectra are also shown in Fig. 2, normalised to one source neutron. Table 2 contains the calculated effective cross-section values and their uncertainties together with calculated ones for $^{252}$Cf.

Table 2. Comparison of results calculated in the present work and those presented in [2] with calculated effective cross-sections in JET DD, DT and $^{252}$Cf neutron spectra.

| Serial No. in IRDFF release 1.05 | Reaction name | Calculated cross section in $^{252}$Cf spontaneous fission $<\sigma_{Cf}>$ (mb) and uncertainty [8] | Calculated effective cross section $<\sigma>$ (mb) and uncertainty | | |
|---|---|---|---|---|---|
| | | | $^{252}$Cf spontaneous fission spectrum | JET DD | JET DT |
| 69 | $^{235}$U(n,f) | 1224.8 ± 0.42 % | 1224.9 ± 0.42 % | 199.69 ± 0.44 % | 148.43 ± 0.42 % |
| 70 | $^{238}$U(n,f) | 318.5 ± 0.66 % | 318.4 ± 0.66 % | 55.26 ± 0.57 % | 53.1 ± 0.56 % |
| 67 | $^{232}$Th(n,f) | 77.56 ± 2.14 % | 79.17 ± 2.15 % | 12.18 ± 2.12 % | 15.61 ± 2.19 % |
| 53 | $^{115}$In(n,n')$^{115m}$In | 190.64 ± 1.70 % | 190.64 ± 1.70 % | 35.27 ± 2.15 % | 12.515 ± 1.43 % |
| 34 | $^{58}$Ni(n,p)$^{58}$Co | 117.5 ± 1.74 % | 117.47 ± 1.89 % | 9.565 ± 2.02 % | 18.006 ± 1.37 % |
| 40 | $^{64}$Zn(n,p)$^{64}$Cu | 42.72 ± 1.86 % | 42.718 ± 1.86 % | 2.88 ± 2.89 % | 7.941 ± 1.37 % |
| 24 | $^{54}$Fe(n,p)$^{54}$Mn | 88.16 ± 2.09 % | 88.151 ± 3.23 % | 5.967 ± 3.37 % | 15.535 ± 3.42 % |
| 31 | $^{59}$Co(n,p)$^{59}$Fe | 1.715 ± 3.65 % | 1.715 ± 6.25 % | 0.007 ± 0.06 % | 1.7475 ± 3.08 % |
| ---- | $^{28}$Si(n,p)$^{28}$Al | N/A | 7.117 ± 0.20 % | ---- | 9.363 ± 0.18 % |
| 26 | $^{56}$Fe(n,p)$^{56}$Mn | 1.475 ± 2.61 % | 1.465 ± 2.98 % | 8.917e-13 ± 8.35 % | 3.766 ± 1.07 % |
| 8 | $^{27}$Al(n,a)$^{24}$Na | 1.019 ± 1.77 % | 1.018 ± 1.77 % | ---- | 4.019 ± 0.40 % |
| 62 | $^{197}$Au(n,2n)$^{196}$Au | 5.531 ± 2.75 % | 5.531 ± 1.52 % | 11.351 ± 7.74 % | 6.787 ± 7.14 % |
| 46 | $^{93}$Nb(n,2n)$^{92m}$Nb | 0.791 ± 2.38 % | 0.791 ± 0.19 % | 0.825 ± 0.46 % | 14.469 ± 0.77 % |
| 36 | $^{63}$Cu(n,2n)$^{62}$Cu | 0.654 ± 3.50 % | 0.694 ± 3.28 % | 9.279e-5 ± 28.74 % | 1.526 ± 1.63 % |
| 44 | $^{90}$Zr(n,2n)$^{89}$Zr | 0.217 ± 5.17 % | 0.217 ± 5.17 % | ---- | 17.63 ± 0.90 % |

## Discussion and conclusions

It can be seen in Table 2 that the uncertainty in the $^{115}$In(n,n')$^{115m}$In, the reaction normally used both in $^{252}$Cf calibrations and with DD plasmas, is 1.70% and 2.15%, respectively. These values are small, as expected, although non negligible. The uncertainties for high threshold reactions used for DT plasmas are all smaller than ~1%, with the only exception of $^{54}$Fe(n,p)$^{54}$Mn and of $^{59}$Co(n,p)$^{59}$Fe for which it amounts to 3.42% and to 3.08%, respectively. The $^{197}$Au(n,2n)$^{196}$Au reaction,

which could be useful in calibration procedures thanks to the high energy threshold and the relatively long half life of the reaction product (9.6 h), is not recommended because of the large uncertainty on the cross section in fusion DT first wall spectrum (7.14%). On the other hand, the newly evaluated $^{28}$Si(n,p)$^{28}$Al reaction, which can be used on a shot by shot basis in DT operations because of the short decay time of its product (2.24 min), is affected by a very small uncertainty (0.18%).These results show that the uncertainties in activation measurements due to the uncertainties in the dosimetric cross sections are generally small, and contribute little to the total

uncertainties in the derived neutron calibration factors. They should however been considered. The tools used in the present work, i.e. activation reactions and covariances data taken from the International Reactor Dosimetry and Fusion File (IRDFF) in 640-groups ENDF-6 form, neutron spectra in the required 640-energy group form, and the RR_UNC code can be used for this purpose.

## Acknowledgments

## References

[1] J. D. Strachan, J. M. Adams, Cris W. Barnes, P. Batistoni, H.S. Bosch et al, Neutron calibration techniques for comparison of tokamak results, Review of Scientific Instruments 61 (1990)

[2] D.B. Syme, S. Popovichev, S. Conroy, I. Lengar, L. Snoj, C. Sowden, L. Giacomelli, G. Hermon, P. Allan, P. Macheta, D. Plummer, J. Stephens, P. Batistoni, R. Prokopowicz, S. Jednorog, M.R. Abhangi, R. Makwana, Fusion yield measurements on JET and their calibration, Fusion Engineering and Design, Volume 89, Issue 11, November 2014, Pages 2766-2775

[3] M. Angelone, P. Batistoni et al., Experimental and numerical calibration of the neutron activation system on the FTU tokamak, Review of Scientific Instruments 61 (1990)

[4] D. B. Syme, S Popovichev, S Conroy, I Lengar, L Snoj, C Sowden, L Giacomelli, G Hermon, P Allan, P Macheta, D Plummer, J Stephens, P Batistoni, Mr R. Prokopowicz, S. Jednorog, M. Abhangi, R Makwa, The JET Neutron Calibration 2013 and its Results, Fusion Engineering Design 2014

[5] P. Batistoni, J. Likonen, N. Bekris, S. Brezinsek, P. Coad, L. Horton, G. Matthews, M. Rubel, G. Sips, B. Syme, A. Widdowson, The JET technology program in support of ITER, accepted for publication in Fusion Engineering and Design (2014)

[6] M. Sasao, L. Bertalot, M. Ishikawa, and S. Popovichev, Review of Scientific Instruments 81, 10D329 (2010);

[7] https://www-nds.iaea.org/IRDFF/
Eva M. Zsolnay, Roberto Capote Noy, Henk J. Nolthenius, Andrej Trkov, Summary Description of the New International Reactor Dosimetric and Fusion File (IRDFF release 1.0), INDC(NDS)-0616.

[8] International Reactor Dosimetric File 2002 (IRDF-2002), International Reactor Fusion File 2002 (IRDF-2002) International Atomic Energy Agency, 2006. Technical reports series, ISSN 0074–1914; 452.

[9] Andrej Trkov, Reactor Physics Division, Jozef Stefan Institute, Ljubljana, Slovenia (private communication), 2013.

[10] Evaluated Nuclear Data File (ENDF), https://www-nds.iaea.org/exfor/endf.htm.

[11] X-5 Monte Carlo Team, MCNP - A General Monte Carlo N-Particle Transport Code, Version 5, Volume I: Overview and Theory (2003) Los Alamos National Lab, Los Alamos